Received: 10 December 2021 | Revised: 8 March 2022 | Accepted: 19 March 2022

DOI: 10.1002/jcla.24383

RESEARCH ARTICLE

WILEY

Decrease in LINC00963 attenuates the progression of pulmonary arterial hypertension via microRNA-328-3p/profilin 1 axis

Chengpeng Yang[1] | Rong Rong[2] | Yuze Li[3] | Mingxun Cheng[4] | Yanzhuo Luo[5]

[1]Cardiothoracic Surgery, First Affiliated Hospital of Jiamusi University, Jiamusi City, China

[2]Department of Physics Diagnosis, First Affiliated Hospital of Jiamusi University, Jiamusi City, China

[3]Department of Nephrology, First Affiliated Hospital of Jiamusi University, Jiamusi City, China

[4]Vascular Surgery, First Affiliated Hospital of Jiamusi University, Jiamusi City, China

[5]Ministry of Continuing Education, First Affiliated Hospital of Jiamusi University, Jiamusi City, China

Correspondence
Yanzhuo Luo, Ministry of Continuing Education, First Affiliated Hospital of Jiamusi University, No. 348, Dexiang Street, Xiangyang District, Jiamusi City, Heilongjiang Province, 154002, China.
Email: bi78094580@163.com

Abstract

Background: Pulmonary arterial hypertension (PAH) is a severe cardiopulmonary disease characterized by vascular hyperplasia and remodeling. Long noncoding RNA LINC00963 can regulate cell proliferation and metastasis in nonsmall cell lung cancer. However, the function of LINC00963 on PAH progression is rarely reported.

Methods: Quantitative real-time PCR was used to determine the expression levels of LINC00963, microRNA (miRNA)-328-3p, and profilin 1 (PFN1), as well as vascular endothelial growth factor (VEGF), fibroblast growth factor 2 (FGF-2), and hypoxia-inducible factor (HIF)-α. The protein level of PFN1 was measured by western blotting. The viability and migration of hypoxia-induced pulmonary arterial smooth muscle cells (PASMCs) were assessed by 3-(4, 5-dimethyl-2-thiazolyl)-2, 5-diphenyl-2-h-tetrazolium bromide, and transwell assays, respectively. The target relationships between miR-328-3p and LINC00963/PFN1 were confirmed by dual-luciferase reporter assay. A PAH mouse model was conducted to explore the effects of hypoxia on cardiopulmonary functions.

Results: In hypoxia-induced PASMCs and PAH mouse model, high expression levels of LINC00963 and PFN1, and low expression of miR-328-3p, were determined. The viability, migration of hypoxia-induced PASMCs, the expression of VEGF, FGF-2, and HIF-α were significantly repressed by transfection of si-LINC00963 or miR-328-3p mimics. The inhibitory effects of LINC00963 silencing on cell viability, migration, and the levels of VEGF, FGF-2, and HIF-α were partly eliminated by miR-328-3p inhibitor or increasing the expression of PFN1. Hypoxia treatment increased the levels of RVSP, mPAP, and RV/(LV+S), as well as the thickness of pulmonary artery wall.

Conclusions: Silencing of LINC00963 ameliorates PAH via modulating miR-328-3p/PFN1.

KEYWORDS
LINC00963, miR-328-3p, PFN1, pulmonary arterial hypertension

1 | INTRODUCTION

Pulmonary arterial hypertension (PAH) is a severe cardiopulmonary disease, and generally caused by various factors such as genetic, epigenetic, and environmental factors.[1–3] Besides, hypoxia is a main inducement to trigger pulmonary vasoconstriction and vascular remodeling, as well as causing hyperplasia and damage to the blood vessels in lungs, eventually resulting in PAH.[3–5] Therefore, exploring the potential mechanisms of vascular hyperplasia and remodeling under hypoxia conditions may be helpful for the treatment of PAH.

Long noncoding RNAs (lncRNAs) are a group of transcripts with 200 nucleotides in length.[6] Wang et al. conducted a microarray analysis for the expression levels of lncRNAs in a PAH rat model and revealed that 86 lncRNAs are abnormally expressed in the progression of PAH.[7] Lei et al. demonstrated that lncRNA is enriched in serum of PAH patients and hypoxia-induced pulmonary arterial smooth muscle cells (PASMCs).[8] Additionally, overexpression of Ang362 is also found in both in vivo and in vitro PAH models.[9] Metastasis-associated lung adenocarcinoma transcript 1 (MALAT1) expression is increased in PAH tissues and in PASMCs isolated from PAH patients, whereas silencing of MALAT1 suppresses the cell proliferation and metastasis.[10] In terms of lncRNA LINC00963, its regulatory role in cellular processes has been reported in multiple human cancers, such as prostate cancer,[11] bladder cancer,[12] ovarian cancer,[13] colorectal cancer,[14] liver cancers,[15] and osteosarcoma.[16] LINC00963 is also confirmed to be closely associated with cell proliferation and metastasis in nonsmall cell lung cancer (NSCLC).[17] Given that the important features of PAH are related to vascular remodeling and hyperplasia, the hypothesis that LINC00963 may be closely associated with the progression of PAH was conducted.

MicroRNAs (miRNAs) are a class of 20–25 nucleotides small endogenous RNA.[18] The increased expression of miR-19a,[19] miR-30a-5p,[20] miR-132,[21] and miR-629[22] is found in PAH, and can aggravate the progression of PAH. On the contrary, there are also many miRNAs exhibiting anti-PAH roles through suppressing cellular processes of PASMCs.[23–25] For instance, increased miR-204 impedes the development of PAH by reducing autophagy.[23] miR-374c can inhibit the viability and metastasis of PASMCs.[24] Overexpression of miR-483 targets PAH-related genes (TGF-β, TGFBR2, and ET-1) to repress right ventricular hypertrophy, indirectly attenuating PAH progression.[25] Notably, up-regulation of miR-328-3p can restrain the proliferation and metastasis of PASMCs, as well as inhibiting vasoconstriction and remodeling via targeting IGF1R, finally ameliorating PAH.[26–28] However, whether miR-328-3p can be modulated by LINC00963 to affect PAH progression has not been reported.

In the current study, the expression of LINC00963, miR-328-3p, and profilin 1 (PFN1) in PAH (in vitro and in vivo models), as well as their interactions in PAH progression in vitro were explored. Our findings may provide a new target for the treatment of PAH.

2 | MATERIAL AND METHODS

2.1 | Cell culture, hypoxia induction, and transfection

Pulmonary arterial smooth muscle cells obtained from BioVector NTCC were cultured in Dulbecco's Modified Eagle's Medium (DMEM) containing 10% fetal bovine serum (FBS). Cells were further divided into two groups: the normoxia group (treatment with 5% CO_2, 21% O_2, and 74% N_2) and the hypoxia group (treatment with 5% CO_2 and 95% N_2). Afterward, siRNA-LINC00963 (si-LINC00963) and its negative control (si-NC) (Transheep), pcDNA3.1-PFN1 vector (pcDNA-PFN1), and pcDNA-NC (Beina Biology), as well as miR-328-3p mimics/mimics NC and miR-328-3p inhibitor/inhibitor NC (Beina Biology) were co-transfected with the hypoxia-induced PASMCs using Lipofectamine RNAiMAX kit (Invitrogen) for 48 h.

2.2 | Quantitative real-time PCR

Total RNA was extracted from PASMCs or lung tissues by RNA extraction kit (Promega), followed by synthesizing into cDNA using First-Strand cDNA Synthesis Kit (Thermo Fisher Scientific). Quantitative real-time PCR was performed with SYBR Green FAST Mastermix (Qiagen). The expression levels of LINC00963, miR-328-3p, PFN1, VEGF, FGF-2, and HIF-1α were quantified by a $2^{-\Delta\Delta Ct}$ method. GAPDH and U6 were served as the internal controls.

2.3 | 3-(4, 5-dimethyl-2-thiazolyl)-2, 5-diphenyl-2-h-tetrazolium bromide assay

Pulmonary arterial smooth muscle cells (1×10^5 cells/μl) were cultured into 96-well plates for 2 days. Subsequently, the cells were incubated for 24, 48, and 72 h, followed by adding 15 μl 3-(4, 5-dimethyl-2-thiazolyl)-2, 5-diphenyl-2-h-tetrazolium bromide (MTT; Aladdin) into each well to incubate another 2 h at 37°C. Cell viability (OD450) was detected using a microplate reader (Thermo Fisher Scientific).

2.4 | Transwell migration assay

The migration of hypoxia-induced PASMCs was measured by transwell assay. In brief, the hypoxia-induced PASMCs (5×10^4) were resuspended in a serum-free DMEM and then seeded into the upper chamber. The lower chamber was added with DMEM containing 10% FBS. Following incubation for overnight at 37°C, cells in the lower chamber were stained with 0.1% crystal violet for 15 min. A light microscope (magnification ×400) was used to count the stained cells in five randomly selected fields.

2.5 | Dual-luciferase reporter assay

The binding sites between miR-328-5p and LINC00963/PFN1 were predicted using StarBase software (http://starbase.sysu.edu.cn/index.php) and TargetScan software (http://www.targetscan.org/vert_72/). Target relationship was further validated by dual-luciferase reporter (DLR) assay. Briefly, the fragments of LINC00963/PFN1 containing miR-328-3p-binding sites were combined with pGL3 vector (Promega) to establish the recombinant reporter plasmids, named LINC00963/PFN1-wild type (WT) or LINC00963/PFN1-mutant type (MUT). We then cotransfected PASMCs (2000 cells per well) with miR-328-3p mimics/mimics NC, and LINC00963/PFN1-WT as well as LINC00963/PFN1-MUT using Lipofectamine 3000 (Thermo Fisher Scientific) to incubate 48 h 37°C. The luciferase activity was analyzed using a dual-luciferase reporter gene assay system (Promega).

2.6 | Western blot assay

Pulmonary arterial smooth muscle cells or lung tissues were initially lysed with RIPA buffer. Afterward, the protein was separated by 10% SDS-PAGE and then transferred onto PVDF membrane, followed by incubating with the primary antibodies PFN1 (1:1000; Sigma Aldrich) and GAPDH (1:1000; Sigma Aldrich) overnight at 4°C and the HRP-conjugated secondary antibody (1:5000; Sigma Aldrich) for 1 h. Immunoblotting was visualized using an ECL detection kit (Thermo Fisher Scientific) under Gel-Pro analyzer version 4.0 (Media Cybernetics).

2.7 | PAH mouse model

C57BL/6 mice (22–24 g) were assigned into two groups ad libitum: the normoxia group ($n = 18$) and hypoxia group ($n = 18$). The normoxia group mice were maintained with the normoxic condition of fractional inspired oxygen 0.21 (FiO_2, 0.21) under a 12 h cycle (12 h for light and 12 h for dark) at 24°C, whereas mice in the hypoxia group were given the hypoxic condition with FiO_2 at 0.12. All animal experiments in this study were in strict accordance with the protocols stated in the Guide for the Care and Use of Laboratory Animals and approval by the ethical committee of First Affiliated Hospital of Jiamusi University.

2.8 | Hemodynamics analysis

The mice were anaesthetized by intraperitoneal injection of pentobarbital sodium (50 mg/kg) at 7, 14, and 21 days, respectively, followed by fixing on an operating table and incising open to expose the diaphragm. A catheter was then slowly inserted from the right external jugular vein. The mice were excluded if insertion of the catheter resulted in perforation of the vessel wall, or if the mice died prematurely. The pressure transducer was connected and a physiological instrument was employed to detect the right ventricular systolic pressure (RVSP) and mean pulmonary artery pressure (mPAP). After measurement, the heart and lung tissues were removed at once, and the right ventricle and left ventricle and ventricular septum were disjointed. Finally, the right ventricle (RV) and left ventricle+ventricular septum (LV+S) were weighed, and the right ventricular hypertrophy index (RVHI) was expressed as RV/(LV+S). The lung tissues were used to perform the subsequent hematoxylin-eosin (H&E) staining assay. Experimenters were blind to the group assignment and did not participate in the later data analysis.

2.9 | H&E staining assay

The fresh lung samples of mice were fixed in 4% paraformaldehyde for one day. Subsequently, lung samples were embedded in paraffin sectioned at 6 μm thickness. The sections were stained with H&E staining immediately and then were observed by light microscopy.

2.10 | Statistical analysis

Data were presented as means ± *SD*. All the experiments in this study were performed in three independent trails. SPSS 20.0 software was used for statistical analysis. Student's *t* test and one-way ANOVA followed by Tukey's multiple comparisons test were used to assess the experimental data. Significant difference was considered when $p < 0.05$.

3 | RESULTS

3.1 | Down-regulation of LINC00963 suppresses PAH progression in vitro

As shown in Figure 1A, we demonstrated that LINC00963 expression was up-regulated by hypoxia treatment in a time-dependent manner ($p < 0.01$). We then silenced LINC00963 to explore its function in PAH progression. The results of transfection efficiency experiments demonstrated that LINC00963 expression was reduced in hypoxia-induced PASMCs by transfection of si-LINC00963 (Figure 1B; $p < 0.01$). As illustrated in Figure 1C–E, cell viability, migration, and the levels of VEGF, FGF-2, and HIF-1α were significantly elevated in hypoxia-induced PASMCs transfected with si-NC ($p < 0.001$), whereas they were partly eliminated by transfection of si-LINC00963 ($p < 0.01$).

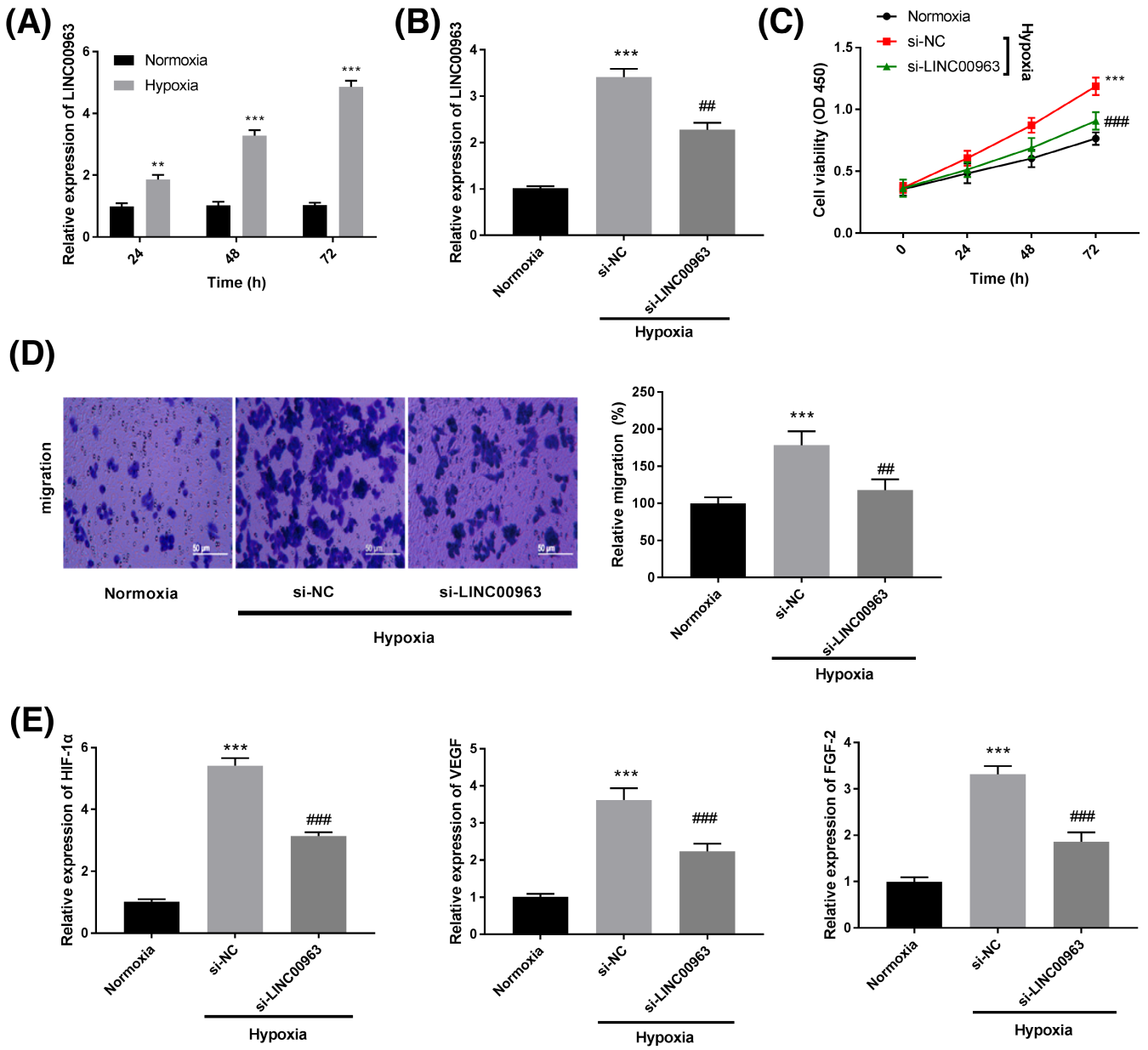

FIGURE 1 Down-regulation of LINC00963 suppresses PAH progression in vitro. (A) LINC00963 expression of hypoxia-induced PASMCs was detected by qRT-PCR. $^{**}p < 0.01$, $^{***}p < 0.001$ versus normoxia PASMCs. (B) LINC00963 expression was detected by qRT-PCR. (C) MTT assay was used to detect the viability (OD450) in different groups. (D) Cell migration was analyzed by wound healing. (E) The expression of HIF-1α, VEGF, and FGF-2 was detected by qRT-PCR. $^{***}p < 0.001$ versus the normoxia group. $^{\#\#}p < 0.01$, $^{\#\#\#}p < 0.001$ versus the si-NC group. FGF-2, fibroblast growth factor 2; HIF-1α, hypoxia-inducible factor 1α; MTT, 3-(4, 5-dimethyl-2-thiazolyl)-2, 5-diphenyl-2-h-tetrazolium bromide; PAH, pulmonary arterial hypertension; PASMC, pulmonary arterial smooth muscle cell; qRT-PCR, quantitative real-time PCR; VEGF, vascular endothelial growth factor

3.2 | MiR-328-3p, a target of LINC00963, plays an inhibitory role in PAH in vitro

The predicted binding site between LINC00963 and miR-328-3p was presented in Figure 2A. DLR assay indicated that the luciferase activity was reduced in the LINC00963-WT/miR-328-3p mimics group compared to the LINC00963-WT/mimics NC group (Figure 2B; $p < 0.01$). Meanwhile, miR-328-3p expression was remarkably increased by si-LINC00963 in hypoxia-induced PASMCs (Figure 2C; $p < 0.01$). Additionally, we found that miR-328-3p expression was decreased by hypoxia treatment in a time-dependent manner (Figure 2D; $p < 0.01$). To elucidate the biological functions of miR-328-3p in progression of PAH in vitro, miR-328-3p was initially overexpressed by transfection of miR-328-3p mimics (Figure 2E; $p < 0.001$), and was repressed by miR-328-3p inhibitor (Figure 2E; $p < 0.05$). As illustrated in Figure 2F–H, miR-328-3p overexpression significantly suppressed cell viability ($p < 0.001$), migration ($p < 0.01$), and the levels of VEGF, FGF-2 and HIF-1α in hypoxia-induced PASMCs ($p < 0.01$).

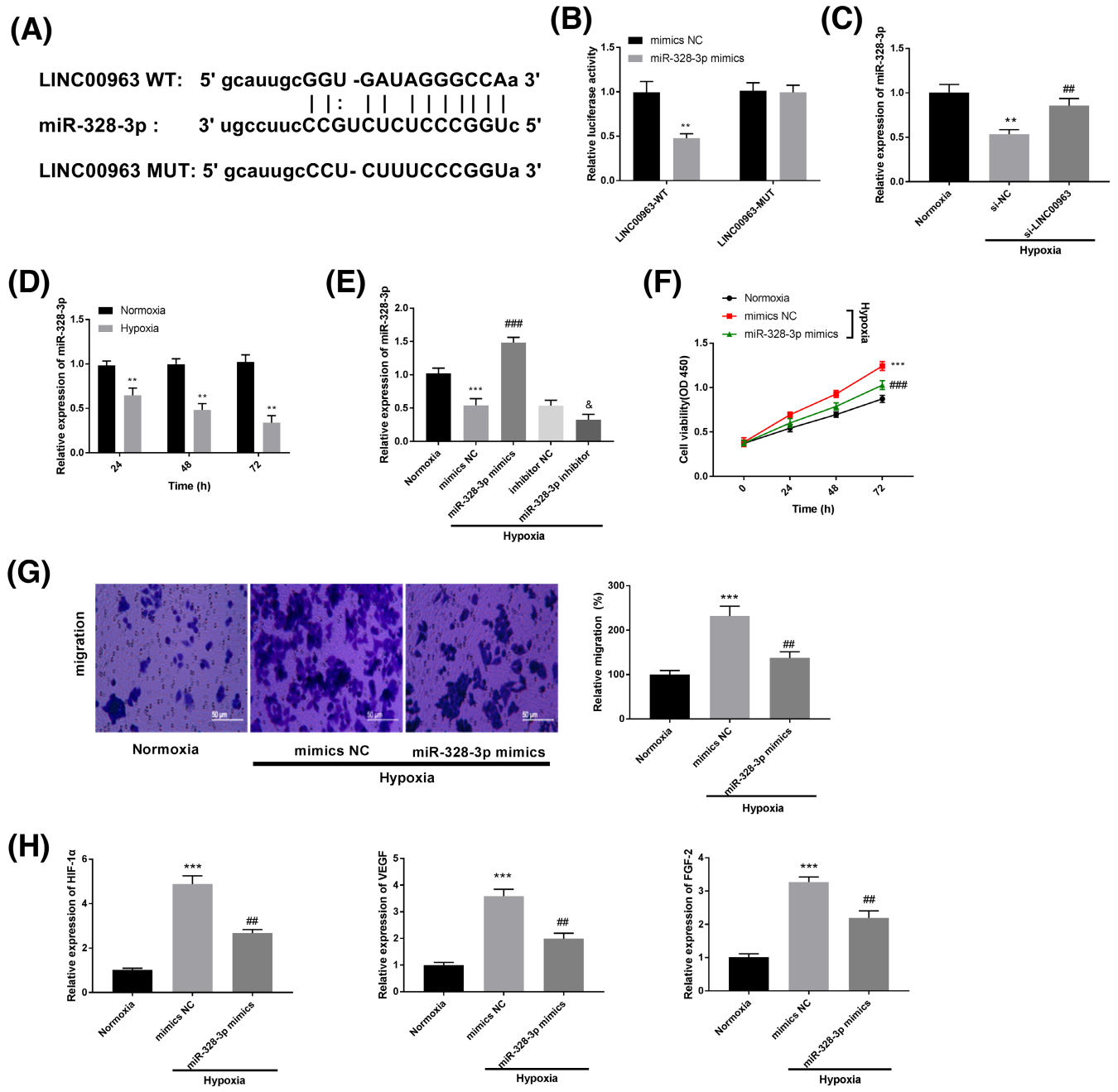

FIGURE 2 MiR-328-3p, a target of LINC00963, plays an inhibitory role in PAH in vitro. (A) The target site between LINC00963 and miR-328-3p was predicted by StarBase. (B) DLR assay confirmed the target relationship between LINC00963 and miR-328-3p in PASMCs. $^{**}p < 0.01$, versus mimics NC. (C) The expression of miR-328-3p was detected by qRT-PCR $^{**}p < 0.01$ versus the normoxia group. $^{\#\#}p < 0.01$ versus the si-NC group. (D) miR-328-3p expression of hypoxia-induced PASMCs was detected by qRT-PCR. $^{**}p < 0.01$ versus normoxia PASMCs. (E) The expression of miR-328-3p was detected by qRT-PCR. $^{***}p < 0.001$ versus the normoxia group. $^{\#\#\#}p < 0.001$ versus the mimics NC group. $^{\&}p < 0.05$ versus the inhibitor NC group. (F) MTT assay was used to detect the viability (OD450) of hypoxia-induced. (G) Cell migration was analyzed by wound-healing assay. (H) The expression of HIF-1α, VEGF, and FGF-2 was detected by qRT-PCR. $^{***}p < 0.001$ versus the normoxia group. $^{\#\#}p < 0.01$, $^{\#\#\#}p < 0.001$ versus the mimics NC group. DLR, dual-luciferase reporter; FGF-2, fibroblast growth factor 2; HIF-1α, hypoxia-inducible factor 1α; PAH, pulmonary arterial hypertension; PASMC, pulmonary arterial smooth muscle cell; qRT-PCR, quantitative real-time PCR; VEGF, vascular endothelial growth factor

3.3 | PFN1 is a target gene of miR-328-3p

A potential binding site between miR-328-3p and PFN1 was shown in Figure 3A. Based on the results of DLR assay, we demonstrated that the luciferase activity of PFN1-WT was significantly decreased with the participation of miR-328-3p mimics, whereas there seemed to be no influences on PFN1-MUT (Figure 3B; $p < 0.01$). Western blotting further demonstrated that PFN1 protein level was repressed in

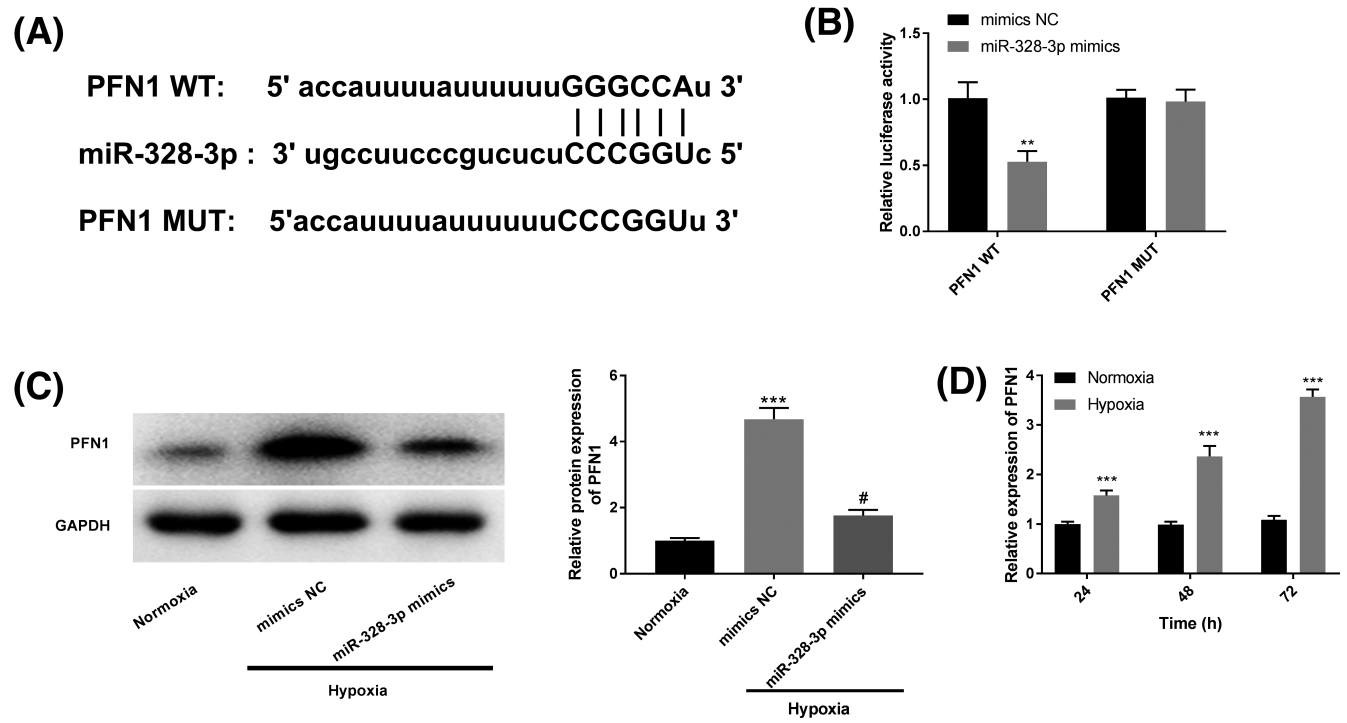

FIGURE 3 PFN1, determined as a target gene of miR-328-3p, is up-regulated in hypoxia-induced PASMCs. (A) The target site between PFN1 and miR-328-3p was predicted by TargetScan. (B) DLR assay confirmed the target relationship between PFN1 and miR-328-3p in PASMCs. $^{**}p < 0.01$, versus mimics NC. (C) The protein level of PFN1 was determined by western blot assay. $^{***}p < 0.001$ versus the normoxia group. $^{\#}p < 0.05$ versus the mimics NC group. (D) PFN1 expression of hypoxia-induced PASMCs was detected by qRT-PCR. $^{***}p < 0.001$ versus normoxia PASMCs. DLR, dual-luciferase reporter; PASMC, pulmonary arterial smooth muscle cell; PFN1, profilin 1; qRT-PCR, quantitative real-time PCR

hypoxia-induced PASMCs after transfection with miR-328-3p mimics (Figure 3C; $p < 0.05$). In addition, we also found an enhanced expression of PFN1 in hypoxia-induced PASMCs (Figure 3D; $p < 0.001$).

3.4 | The inhibitory role of LINC00963/miR-328-3p/PFN1 axis in PAH in vitro

Profilin 1 was overexpressed by transfection of pcDNA-PFN1 into hypoxia-induced PASMCs to investigate the function of PFN1 in PAH progression (Figure 4A; $p < 0.001$). Western blot assay uncovered that the protein level of PFN1 was inhibited by LINC00963 knockdown (Figure 4B; $p < 0.05$), but was rescued via miR-328-3p down-regulation (Figure 4B; $p < 0.01$). As illustrated in Figure 4C–E, we revealed that miR-328-3p inhibitor or pcDNA-PFN1 reversed the suppressive effects of si-LINC00963 on cell viability, migration, and the levels of VEGF, FGF-2, and HIF-1α in hypoxia-induced PASMCs ($p < 0.01$).

3.5 | Hypoxia promotes pulmonary vascular remodeling

In a PAH mouse model, we discovered that the levels of RVSP, mPAP, and the ratio of RV/(LV+S) (Figure 5A; $p < 0.01$) as well as the thickness of pulmonary artery wall (Figure 5B) were significantly increased in a time-dependent manner. Meantime, the expression levels of LINC00963, miR-328-3p, and PFN1 in lung tissues of PAH mice were also detected, indicating that the expression levels of LINC00963 and PFN1 were up-regulated, whereas miR-328 expression level was down-regulated (Figure 5C–E; $p < 0.01$).

4 | DISCUSSION

Pulmonary arterial hypertension, a life-threatening cardiopulmonary disease, is characterized by pulmonary vasculature remodeling and vasculopathy. It can lead to a sustained rise in pulmonary arterial pressure, heart failure, and even death.[29] A hypoxia-induced murine PAH model is usually established to explore the progression of PAH in vivo.[26,30] In our study, the levels of RVSP, mPAP, and RV/(LV+S) ratio, as well as the thickness of the pulmonary artery wall were all significantly increased in hypoxia-induced PAH mice, suggesting that the PAH mouse model was successfully conducted in this study. Recently, numerous studies have reported that lncRNAs are strongly associated with the occurrence and development of PAH.[31–34] Some lncRNAs are down-regulated in PAH, including CPS1-IT,[31] ANRIL,[32] and CASC2.[33] More importantly, also some lncRNAs are found to overexpress in PAH, such as Ang362[9] and UCA1,[34] indicating the pathogenic role in the pathogenesis of PAH. In the present study, we

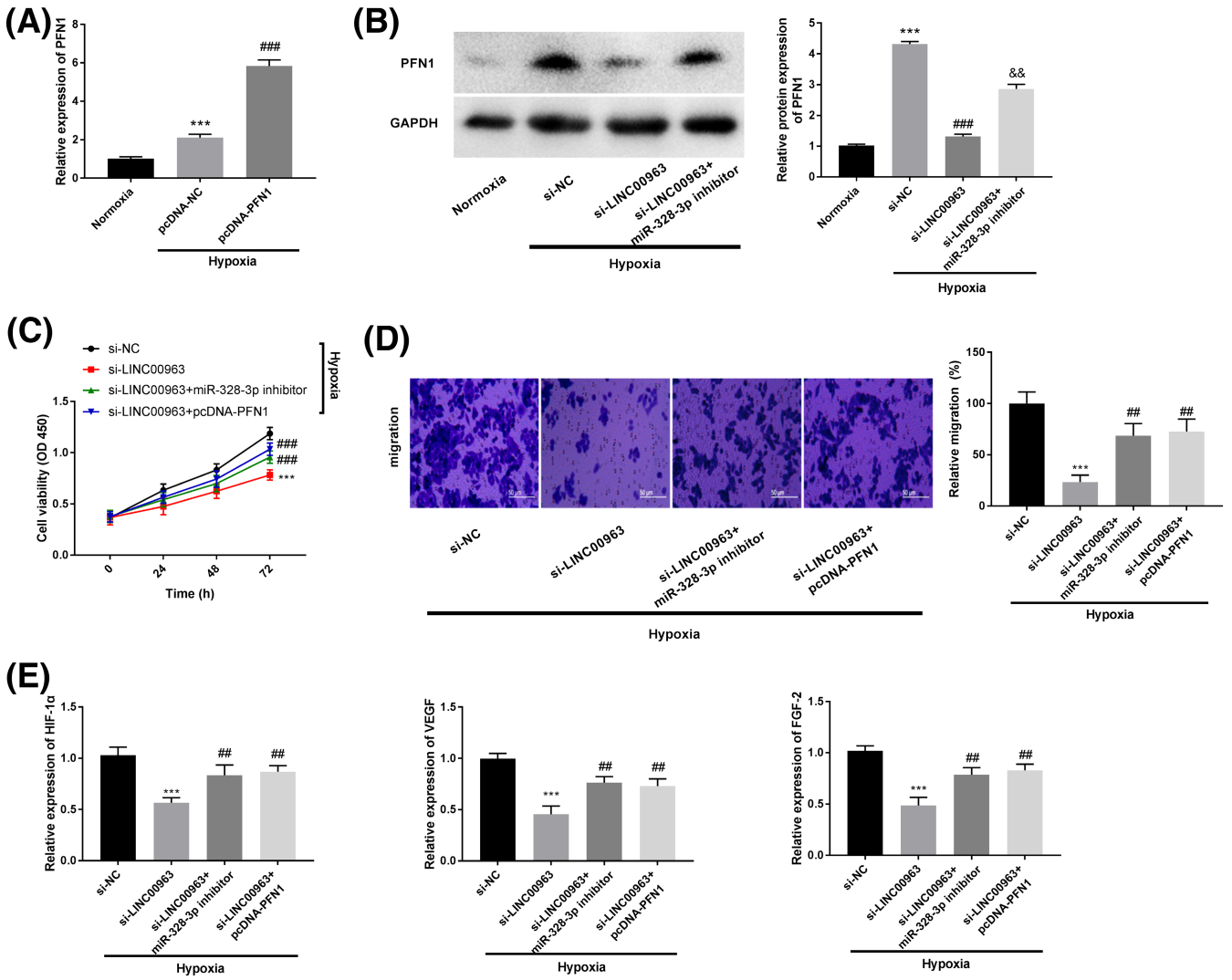

FIGURE 4 The inhibitory role of LINC00963/miR-328-3p/PFN1 axis in PAH in vitro. (A) PFN1 expression was detected by qRT-PCR in hypoxia-induced pulmonary arterial smooth muscle cells transfected with pcDNA-NC or pcDNA-PFN1. $^{***}p < 0.001$ versus the normoxia group. $^{###}p < 0.001$ versus the pcDNA-NC group. (B) The protein level of PFN1 was determined by western blot assay. $^{&&}p < 0.01$ versus the si-LINC00963 group. (C) The viability was detected by MTT assay. (D) Cell migration was analyzed by wound-healing assay. (E) The expression of HIF-1α, VEGF, and FGF-2 was detected by RT-qPCR. $^{***}p < 0.001$ versus the si-NC group. $^{##}p < 0.01$, $^{###}p < 0.001$ versus the si-LINC00963 group. FGF-2, fibroblast growth factor 2; HIF-1α, hypoxia-inducible factor 1α; MTT, 3-(4, 5-dimethyl-2-thiazolyl)-2, 5-diphenyl-2-h-tetrazolium bromide; PAH, pulmonary arterial hypertension; PFN1, profilin 1; qRT-PCR, quantitative real-time PCR; VEGF, vascular endothelial growth factor

indicated that LINC00963 expression was increased both in hypoxia-induced PASMCs and PAH mouse model in a time-dependent manner. Therefore, we speculated the LINC00963 may be a pathogenic factor in the occurrence of PAH.

As the previous studies described, inhibition of Ang362 or MALAT1 significantly reduced the viability and metastasis of hypoxia-induced PASMCs.[9,10] In this study, we also discovered a phenomenon that the low expression level of LINC00963 has inhibiting effects on cell viability and migration. Interestingly, Yu et al. focused on the function of LINC00963 on NSCLC and found that the metastasis of NSCLC cells can be suppressed by transfection of si-LINC00963, thus ameliorating NSCLC. Based on the similar influences of LINC00963 on cell viability and migration in PAH and NSCLC, respectively, we further speculated that silencing of LINC00963 may also repress PAH progression via inhibition of hypoxia-induced PASMCs proliferation and migration. At the same time, silencing of LINC00963 also exerted an inhibitory effect on vascular remodeling, which serves as an important feature of PAH. Therefore, we believed that silencing of LINC00963 repressed the development of PAH via controlling the excessive hyperplasia of PASMCs.

Several miRNAs are decreased in PAH tissues or hypoxia-stimulated PASMCs, such as miR-141,[8] miR-204,[23] miR-374c,[24] miR-483.[25] Besides, overexpression of these miRNAs can remarkably suppress the development of PAH.[8,23–25] Herein, a reduction of miR-328-3p expression was also determined. Interestingly, high

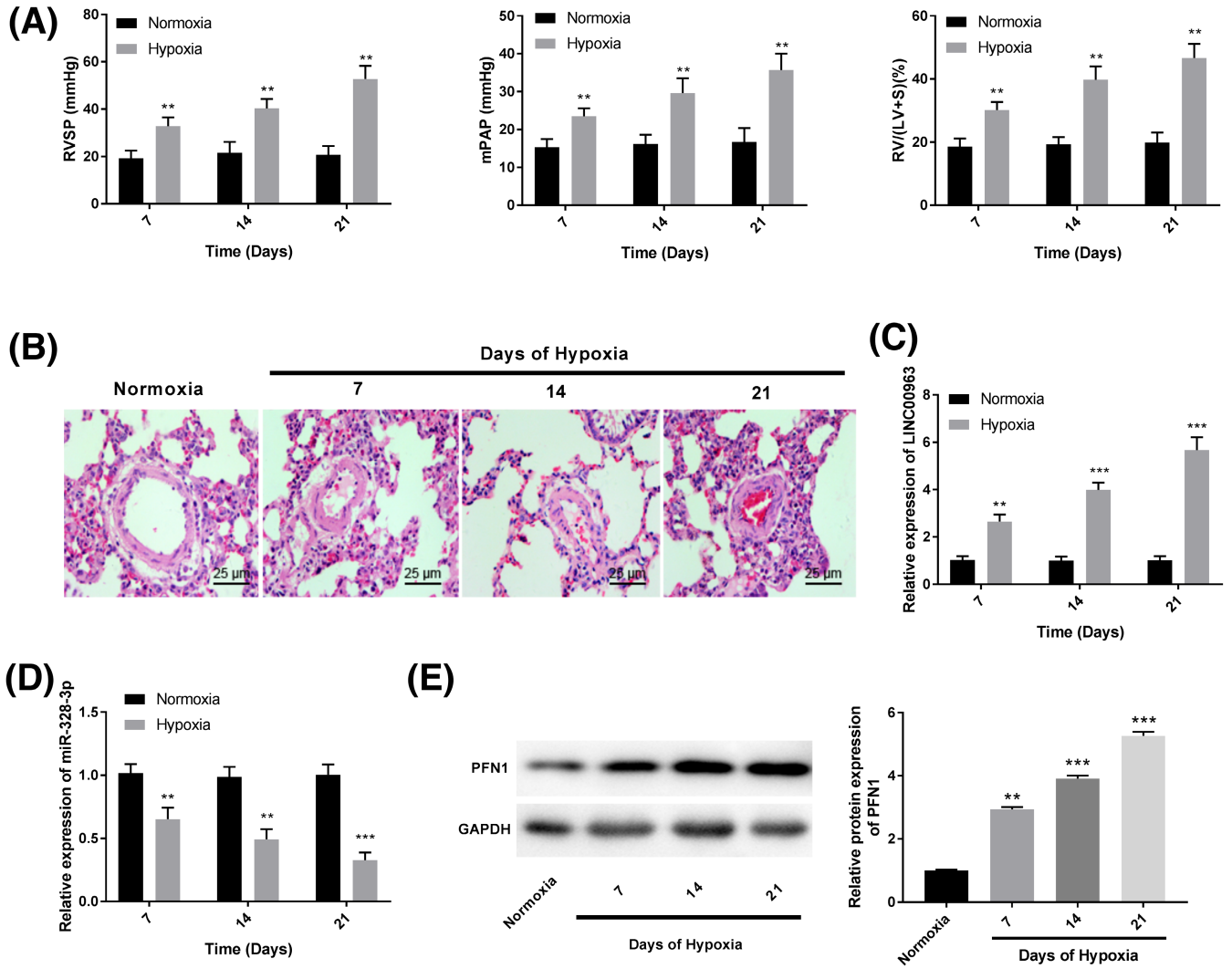

FIGURE 5 Hypoxia induction promotes pulmonary vascular remodeling. (A) The levels of RVSP, mPAP, and the ratio of RV/(LV+S) of hypoxia-induced PAH mice were detected by a physiological instrument. $^{**}p < 0.01$ versus normoxia mice. (B) hematoxylin-eosin was utilized for staining lung tissues of mice to evaluate morphological changes in lungs after hypoxia induction. (C) The expression of LINC00963 in hypoxia-induced mice was detected by qRT-PCR. (D) The expression of miR-328-3p in hypoxia-induced mice was detected by qRT-PCR. (E) The protein level of PFN1 in hypoxia-induced mice was determined by western blot assay. $^{**}p < 0.01$, $^{***}p < 0.001$ versus normoxia mice. LV+S, left ventricle+ventricular septum; mPAP, mean pulmonary artery pressure; PAH, pulmonary arterial hypertension; PFN1, profilin 1; qRT-PCR, quantitative real-time PCR; RV, right ventricle; RVSP, right ventricular systolic pressure

expression level of miR-328-3p also inhibited cell viability and migration. Our results lend credence to the previous study suggesting that miR-328-3p overexpression impedes the proliferation and migration of hypoxia-induced PASMCs.[26] Besides, we further demonstrated that miR-328-3p overexpression attenuates the levels of VEGF, FGF-2, and HIF-α. All the results suggested that up-regulation of miR-328-3p may inhibit vasculature hyperplasia and remodeling, and finally retard the occurrence of PAH. Additionally, miR-328-3p was identified as a downstream target of LINC00963. We suggested that LINC0963 may act as a sponge of miR-328-3p in PAH progression. As expected, we found the suppressive effects of LINC00963 silencing on viability, migration, and the levels of VEGF, FGF-2, and HIF-α were rescued by miR-328-3p inhibition. The results suggested that silencing of LINC00963 affects PAH by modulating miR-328-3p.

Profilin 1, a widely expressed actin-binding protein, is essential for normal cell motility, proliferation, and differentiation.[35] High expression of PFN1 is determined in multiple human cardiopulmonary diseases, such as lung cancer,[36] allergic airway,[37] asthma,[38] and acute myocardial infarction.[39] In the current study, the expression level of PFN1 was increased in both hypoxia-treated PASMCs and PAH mouse model. In line with our findings, Dai et al. have reported an enhanced expression of PFN1 in platelet-derived growth factor and IL-1β cocultured PASMCs and monocrotaline-induced rat model.[40] The results implied that high expression of PFN1 is closely associated with the exacerbation of PAH. Meanwhile, PFN1 is found to be the downstream target of miR-328-3p. Therefore, we further made a hypothesis that the LINC00963/miR-328-3p axis may interact with PFN1 to affect PAH. Our rescue experiments demonstrated

that overexpression of PFN1 reversed the inhibiting effects of LINC00963 knockdown on viability, migration, and the levels of VEGF, FGF-2, and HIF-α. Taken together, we considered that silencing of LINC00963 can attenuate PAH through sponging miR-328-3p and mediating PFN1.

There are some unsolved research topics we need to elucidate in the future. First, the animal experiment should be performed to validate the effects of LINC00963/miR-328-3p/PFN1 in vivo. Second, further clinical experiments are required to determine whether LINC00963 can be a therapeutic target for PAH.

5 | CONCLUSION

In summary, increased LINC00963 and PFN1, as well as decreased miR-328-3p, were found in PAH. Silencing of LINC00963 represses the development of PAH via regulating the miR-328-3p/PFN1 axis, pointing out a novel potential target for PAH therapy.

CONFLICT OF INTEREST

No conflicts of interest have been declared.

AUTHOR CONTRIBUTIONS

Chengpeng Yang and Mingxun Cheng were mainly responsible for concept design, investigation, and research; Yanzhuo Luo conducted data analysis and interpretation and provided administrative support; Rong Rong and Yuze Li were responsible for data collection and experimental operation; Chengpeng Yang wrote the draft of manuscript. All authors reviewed the manuscript.

DATA AVAILABILITY STATEMENT

The datasets used and/or analyzed during the current study are available from the corresponding author on reasonable request.

ORCID

Yanzhuo Luo https://orcid.org/0000-0001-9813-8910

REFERENCES

1. Hong KH, Lee YJ, Lee E, et al. Genetic ablation of the BMPR2 gene in pulmonary endothelium is sufficient to predispose to pulmonary arterial hypertension. *Circulation*. 2008;118(7):722-730.
2. Pullamsetti SS, Perros F, Chelladurai P, Yuan J, Stenmark K. Transcription factors, transcriptional coregulators, and epigenetic modulation in the control of pulmonary vascular cell phenotype: therapeutic implications for pulmonary hypertension (2015 Grover Conference series). *Pulm Circ*. 2016;6(4):448-464.
3. Shimoda LA, Laurie SS. Vascular remodeling in pulmonary hypertension. *J Mol Med*. 2013;91(3):297-309.
4. Nie X, Chen Y, Tan J, et al. MicroRNA-221-3p promotes pulmonary artery smooth muscle cells proliferation by targeting AXIN2 during pulmonary arterial hypertension. *Vascul Pharmacol*. 2019;116:24-35.
5. Lu X, Murphy TC, Nanes MS, Hart CM. PPARγ regulates hypoxia-induced Nox4 expression in human pulmonary artery smooth muscle cells through NF-κB. *Am J Physiol Lung Cell Mol Physiol*. 2010;299(4):L559-566.
6. Klinge CM. Non-coding RNAs: long non-coding RNAs and microRNAs in endocrine-related cancers. *Endocr Relat Cancer*. 2018;25(4):R259-R282.
7. Wang X, Yan C, Xu X, et al. Long noncoding RNA expression profiles of hypoxic pulmonary hypertension rat model. *Gene*. 2016;579(1):23-28.
8. Lei S, Peng F, Li ML, Duan WB, Peng CQ, Wu SJ. LncRNA-SMILR modulates RhoA/ROCK signaling by targeting miR-141 to regulate vascular remodeling in pulmonary arterial hypertension. *Am J Physiol Heart Circ Physiol*. 2020;319(2):H377-H391.
9. Wang H, Qin R, Cheng Y. LncRNA-Ang362 promotes pulmonary arterial hypertension by regulating miR-221 and miR-222. *Shock*. 2020;53(6):723-729.
10. Wang D, Xu H, Wu B, et al. Long noncoding RNA MALAT1 sponges miR1243p.1/KLF5 to promote pulmonary vascular remodeling and cell cycle progression of pulmonary artery hypertension. *Int J Mol Med*. 2019;44(3):871-884.
11. Sun F, Wu KE, Yao Z, et al. Long noncoding RNA LINC00963 induces NOP2 expression by sponging tumor suppressor miR-542-3p to promote metastasis in prostate cancer. *Aging*. 2020;12(12):11500-11516.
12. Zhou N, Zhu X, Man L. LINC00963 Functions as an oncogene in bladder cancer by regulating the miR-766-3p/MTA1 Axis. *Cancer Manag Res*. 2020;12:3353-3361.
13. Liu W, Yang YJ, An Q. LINC00963 promotes ovarian cancer proliferation, migration and EMT via the miR-378g /CHI3L1 axis. *Cancer Manag Res*. 2020;12:463-473.
14. Zheng K, Zhang TK. LncRNA LINC00963 promotes proliferation and migration through the miR-124-3p/FZD4 pathway in colorectal cancer. *Eur Rev Med Pharmacol Sci*. 2020;24(14):7634-7644.
15. Wu JH, Tian XY, An QM, Guan XY, Hao CY. LINC00963 promotes hepatocellular carcinoma progression by activating PI3K/AKT pathway. *Eur Rev Med Pharmacol Sci*. 2018;22(6):1645-1652.
16. Zhou Y, Yin L, Li H, Liu LH, Xiao T. The LncRNA LINC00963 facilitates osteosarcoma proliferation and invasion by suppressing miR-204-3p/FN1 axis. *Cancer Biol Ther*. 2019;20(8):1141-1148.
17. Yu T, Zhao Y, Hu Z, et al. MetaLnc9 facilitates lung cancer metastasis via a PGK1-activated AKT/mTOR pathway. *Can Res*. 2017;77(21):5782-5794.
18. Bartel DP. MicroRNAs: target recognition and regulatory functions. *Cell*. 2009;136(2):215-233.
19. Zhao M, Chen N, Li X, Lin L, Chen X. MiR-19a modulates hypoxia-mediated cell proliferation and migration via repressing PTEN in human pulmonary arterial smooth muscle. *Life Sci*. 2019;239:116928.
20. Tan H, Yao H, Lie Z, Chen G, Lin S, Zhang Y. MicroRNA30a5p promotes proliferation and inhibits apoptosis of human pulmonary artery endothelial cells under hypoxia by targeting YKL40. *Mol Med Rep*. 2019;20(1):236-244.
21. Zeng ZH, Wu WH, Peng Q, Sun YH, Liu JX. MicroRNA132 mediates proliferation and migration of pulmonary smooth muscle cells via targeting PTEN. *Mol Med Rep*. 2019;19(5):3823-3830.
22. Zhao M, Chen N, Li X, Lin L. MiR-629 regulates hypoxic pulmonary vascular remodelling by targeting FOXO3 and PERP. *J Cell Mol Med*. 2019;23(8):5165-5175.
23. Liu T, Zou X-Z, Huang N, et al. Down-regulation of miR-204 attenuates endothelial-mesenchymal transition by enhancing autophagy in hypoxia-induced pulmonary hypertension. *Eur J Pharmacol*. 2019;863:172673.
24. Yang L, Liang H, Shen L, Guan Z, Meng X. LncRNA Tug1 involves in the pulmonary vascular remodeling in mice with hypoxic pulmonary hypertension via the microRNA-374c-mediated Foxc1. *Life Sci*. 2019;237:116769.
25. Zhang J, He Y, Yan X, et al. MicroRNA-483 amelioration of experimental pulmonary hypertension. *EMBO Mol Med*. 2020;12(5):e11303.

26. Xing Y, Zheng X, Fu Y, et al. Long Noncoding RNA-maternally expressed gene 3 contributes to hypoxic pulmonary hypertension. *Mol Ther*. 2019;27(12):2166-2181.
27. Bienertova-Vasku J, Novak J, Vasku A. MicroRNAs in pulmonary arterial hypertension: pathogenesis, diagnosis and treatment. *J Am Soc Hypertens*. 2015;9(3):221-234.
28. Guo L, Qiu Z, Wei L, et al. The microRNA-328 regulates hypoxic pulmonary hypertension by targeting at insulin growth factor 1 receptor and L-type calcium channel-alpha1C. *Hypertension*. 2012;59(5):1006-1013.
29. Rabinovitch M, Guignabert C, Humbert M, Nicolls MR. Inflammation and immunity in the pathogenesis of pulmonary arterial hypertension. *Circ Res*. 2014;115(1):165-175.
30. Liu Y, Sun Z, Zhu J, Xiao B, Dong J, Li X. LncRNA-TCONS_00034812 in cell proliferation and apoptosis of pulmonary artery smooth muscle cells and its mechanism. *J Cell Physiol*. 2018;233(6):4801-4814.
31. Zhang Z, Li Z, Wang Y, Wei L, Chen H. Overexpressed long noncoding RNA CPS1-IT alleviates pulmonary arterial hypertension in obstructive sleep apnea by reducing interleukin-1beta expression via HIF1 transcriptional activity. *J Cell Physiol*. 2019;234(11):19715-19727.
32. Wang S, Zhang C, Zhang X. Downregulation of long noncoding RNA ANRIL promotes proliferation and migration in hypoxic human pulmonary artery smooth muscle cells. *Mol Med Rep*. 2020;21(2):589-596.
33. Han Y, Liu Y, Yang C, Gao C, Guo X, Cheng J. LncRNA CASC2 inhibits hypoxia-induced pulmonary artery smooth muscle cell proliferation and migration by regulating the miR-222/ING5 axis. *Cell Mol Biol Lett*. 2020;25:21.
34. Zhu T-T, Sun R-L, Yin Y-L, et al. Long noncoding RNA UCA1 promotes the proliferation of hypoxic human pulmonary artery smooth muscle cells. *Eur J Physiol*. 2019;471(2):347-355.
35. Mazzatti DJ, Pawelec G, Longdin R, Powell JR, Forsey RJ. SELDI-TOF-MS ProteinChip array profiling of T-cell clones propagated in long-term culture identifies human profilin-1 as a potential biomarker of immunosenescence. *Proteome Sci*. 2007;5:7.
36. Gagat M, Halas-Wisniewska M, Zielinska W, Izdebska M, Grzanka D, Grzanka A. The effect of piperlongumine on endothelial and lung adenocarcinoma cells with regulated expression of profilin-1. *OncoTargets Ther*. 2018;11:8275-8292.
37. Song SM, Kang SA, Park HK, et al. Acanthamoeba profilin elicits allergic airway inflammation in mice. *PLoS Negl Trop Dis*. 2018;12(12):e0006979.
38. Wang R, Cleary RA, Wang T, Li J, Tang DD. The association of cortactin with profilin-1 is critical for smooth muscle contraction. *J Biol Chem*. 2014;289(20):14157-14169.
39. Hao P, Fu K, Wang SP, et al. Expression of profilin-1 in endothelial cells of rats with acute myocardial infarction. *Eur Rev Med Pharmacol Sci*. 2017;21(6):1318-1322.
40. Dai YP, Bongalon S, Tian H, Parks SD, Mutafova-Yambolieva VN, Yamboliev IA. Upregulation of profilin, cofilin-2 and LIMK2 in cultured pulmonary artery smooth muscle cells and in pulmonary arteries of monocrotaline-treated rats. *Vascul Pharmacol*. 2006;44(5):275-282.

How to cite this article: Yang C, Rong R, Li Y, Cheng M, Luo Y. Decrease in LINC00963 attenuates the progression of pulmonary arterial hypertension via microRNA-328-3p/profilin 1 axis. *J Clin Lab Anal*. 2022;36:e24383. doi:10.1002/jcla.24383